On Airborne Doppler Navigation System Application for Measurement of the Water Surface Backscattering Signature and Estimation of the Near-Surface Wind

Alexey Nekrasov*

Taganrog Institute of Technology, Southern Federal University, Taganrog, Russia, Hamburg University of Technology, Hamburg, Germany, and The Ohio State University, Columbus, USA

Abstract: A method for measuring the water surface backscattering signature and estimating the near-surface wind vector over water using the airborne Doppler navigation system in addition to its standard navigational application is discussed. A case of an airplane circle flight measurement of the azimuth normalized radar cross section curve of the water surface in the range of middle incidence angles is considered. The system operates in the scatterometer mode and uses a fore-beam directed to the right side at a typical mounting angle in the vertical plane that is not so far from nadir at a straight flight. Wind vector is recovered from the azimuth normalized radar cross section curve obtained. Algorithms for measuring the water surface backscattering signature and extracting the wind speed and direction are proposed.

Keywords: Doppler navigation system, Scatterometer, Water surface backscattering signature, Sea wind, Algorithm.

INTRODUCTION

On the global scale, the information about sea waves and wind, in general, could be obtained from a satellite using active microwave instruments: Scatterometer, Synthetic Aperture Radar and Radar Altimeter [1]. However, for the local numerical weather and wave models as well as for a pilot on an amphibious airplane to make a landing decision, the local data about wave height, wind speed and direction are required.

Many researchers have been investigating the microwave backscattering signatures of the water surface and solving the problem of remote measuring of the wind speed and direction over water [2-13]. However, the mechanics of interactions between water surfaces and microwaves have not been well studied in detail.

The typical method for describing sea clutter is in the form of the normalized radar cross section (NRCS), the statistical distribution of the NRCS, the amplitude correlation and the spectral shape of the Doppler returns [14].

To describe the radar backscatter from the water surfaces, three major scattering models are used: the Kirchhoff or physical optics model, the composite-surface or two-scale model, and the Bragg model. The Kirchhoff model assumes a perfectly conducting surface (unless it is modified to include the Fresnel reflection coefficient) and applies from small to intermediate incidence angles without shadowing effects. Apart from the implicit dependence on the Fresnel coefficient, there is no polarization dependence. The two-scale model assumes that the radar backscatter arises from a large number of slightly rough ripples, distributed over the long ocean waves. It has polarization dependence. These two models are generally used to interpret the data acquired by the synthetic aperture radar and real aperture radar of a variety of sea/oceanic features, including swell waves and internal waves. The Bragg model applies only to the slightly rough surfaces under low wind conditions (it is often used to describe the scattering from ripples in the two-scale model). The Bragg model has been used to interpret the ocean currents by high-frequency Doppler radar measurements at large incidence angles [15].

To explain adequately the microwave scattering signature of the water surface and to apply its features to remote sensing, a set of experiments, namely, experimental verification of the combined frequency, azimuth and incidence angles, and wind speed variations of the NRCS are required [6]. For that study, a scatterometer, radar designed for measuring the surface scatter characteristics, is used.

Research on microwave backscatter by the water surface has shown that the use of a scatterometer also allows an estimation of near-surface wind vector because the NRCS of the water surface depends on the wind speeds and directions. Based on experimental data and scattering theory, a significant number of empirical and theoretical backscatter models and algorithms for estimation of a near-surface wind vector from satellite and airplane has been developed [16]. The accuracy of the wind direction measurement is ±20°, and the accuracy of the wind speed measurement is ±2 m/s in the wind speed range 3–24 m/s.

Wind blowing over the sea affects the water surface backscatter. Wind speed U can be determined by a scatterometer because a stronger wind will produce a larger

*Address correspondence to this author at the Taganrog Institute of Technology, Southern Federal University, Per. 1 Krepostnoy 34, k. 249, 347922 Taganrog, Russia; Tel: +07 8634 360484;
Fax: +7 8634 310598; E-mail: alexei-nekrassov@mail.ru

1875-4139/12

NRCS $\sigma^{\circ}(U,\theta,\alpha)$ at the middle incidence angle θ. Wind direction can also be inferred because the NRCS varies as a function of the azimuth observation angle α relative to the up-wind direction. To retrieve the wind vector from NRCS measurements, the relationship between the NRCS and near-surface wind, called the "geophysical model function", must be known. Scatterometer experiments have shown that the NRCS model function for middle incidence angles is of the widely used form [17]

$$\sigma^{\circ}(U,\theta,\alpha) = A(U,\theta) + B(U,\theta)\cos\alpha + C(U,\theta)\cos(2\alpha), \quad (1)$$

where $A(U,\theta)$, $B(U,\theta)$ and $C(U,\theta)$ are the Fourier terms that depend on sea surface wind speed and incidence angle, $A(U,\theta) = a_0(\theta)U^{\gamma_0(\theta)}$, $B(U,\theta) = a_1(\theta)U^{\gamma_1(\theta)}$, and $C(U,\theta) = a_2(\theta)U^{\gamma_2(\theta)}$; $a_0(\theta)$, $a_1(\theta)$, $a_2(\theta)$, $\gamma_0(\theta)$, $\gamma_1(\theta)$ and $\gamma_2(\theta)$ are the coefficients dependent on the incidence angle. The $A(U,\theta)$ term equals the azimuthally averaged NRCS; the $B(U,\theta)$ term embodies the upwind-downwind asymmetry; and the $C(U,\theta)$ term represents the upwind-crosswind anisotropy. Detail procedures to obtain the above terms from backscatter values in the upwind, downwind, and crosswind directions have been reported in [18]. The coefficients $a_0(\theta)$, $a_1(\theta)$, $a_2(\theta)$, $\gamma_0(\theta)$, $\gamma_1(\theta)$ and $\gamma_2(\theta)$ are determined empirically for an appropriate geophysical model function using airborne and satellite measurements, and validating surface measurements. The coefficients are tabulated or represented as functions of incidence angle [2, 7, 16, 19].

To study a microwave backscattering signature of the water surface from airplane, an airborne scatterometer is used. The measurements are typically performed at either a circle track flight using fixed fan-beam antenna or a rectilinear track flight using rotating antenna [6, 7, 9, 20]. Unfortunately, a microwave narrow-beam antenna has considerable size at Ku-, X- and C-bands that makes its placing on a flying apparatus difficult. Therefore, a better way needs to be found.

At least two ways can be proposed. The first way is to apply the airborne scatterometers with wide-beam antennas as it can lead to the reduction in the antenna size. The second way is to use the modified conventional navigation instruments of flying apparatus in a scatterometer mode that seems more preferable.

From that point of view, a promising navigation instrument is the Doppler navigation system (DNS). In this connection, a method to measure the water surface backscattering signature and to estimate the wind speed and direction by the airborne DNS operating in the scatterometer mode at aircraft circle flight, in addition to its standard navigation application, is discussed in this paper.

MATERIAL AND METHODS

Doppler Navigation System

DNS is the self-contained radar system that utilizes the Doppler effect (Doppler radar) for measuring the ground speed and drift angle of flying apparatus and accomplishes its dead-reckoning navigation [21]. The internationally authorized frequency band of 13.25 to 13.4 GHz has been allocated for airborne Doppler navigation radar. A center frequency of 13.325 GHz of the band corresponds to a wave length of 2.25 cm. This frequency represents a good compromise between too low a frequency, resulting in low-velocity sensitivity and large aircraft antenna size and beam widths, and too high a frequency, resulting in excessive absorption and backscattering effects of the atmosphere and precipitation. (Earlier Doppler radars operated in two somewhat lower frequency bands, i.e., centered at 8.8 and 9.8 GHz, respectively, but now these bands are no longer used for stand-alone Doppler radars.) [22].

Measurement of the wind vector and drift angle of flying apparatus is based on change of a Doppler frequency of the signal reflected from the underlying surface, depending on a spatial position of an antenna beam. Usually, an antenna of the DNS has three beams (λ-configuration; beams 1, 2, and 3) or four beams (x-configuration; beams 1, 2, 3, and 4) located in space as represented in Fig. (**1**). An effective antenna beamwidth is of 3° to 10° [23]. Power reasons (DNS should operates over water as well as over land) and sensitivity of the DNS to velocity influence a choice of a mounting angle of a beam axis in the vertical plane θ_0.

The NRCS of underlying surface depends on the incidence angle for radar system operating in the frequency band (Ke-band) currently assigned to Doppler navigation radar [22]. For most types of terrain the NRCS decreases slowly with increase of the beam incidence angle. However, for water surfaces, the NRCS falls radically as the incidence angle increases and assumes different values for different conditions of sea state or water roughness. For the typical Doppler-radar incidence angles of 15° to 30° [23], the NRCS is considerably smaller for most sea states than for land and decreases markedly for the smoother sea state. Therefore, a conservative Doppler-radar design is based on an NRCS for the smoothest sea state over which the aircraft is expected to navigate. (Very smooth sea states are relatively rare).

There are two basic antenna system concepts used for drift angle measurement. These are the fixed-antenna system, which is used in most modern systems, and the track-stabilized (roll-and-pitch-stabilized) antenna system. For physically roll-and-pitch-stabilized antenna systems, the value of an incidence angle remains essentially constant and equal to the chosen design value. For fixed-antenna system, a conservative design is based on the NRCS and range for the largest incidence angle that would be expected for the largest combination of pitch and roll angles of the aircraft [22].

The choice of a mounting angle of a beam axis in the inclined plane η_0 (nominal angle between antenna longitudinal axis and central beam direction) represents a compromise between high sensitivity to velocity and over-water accuracy, which increases with smaller mounting angles of a beam axis in the inclined plane, and high signal return over water, which increases for larger mounting angles of a beam axis in the inclined plane. Most equipments

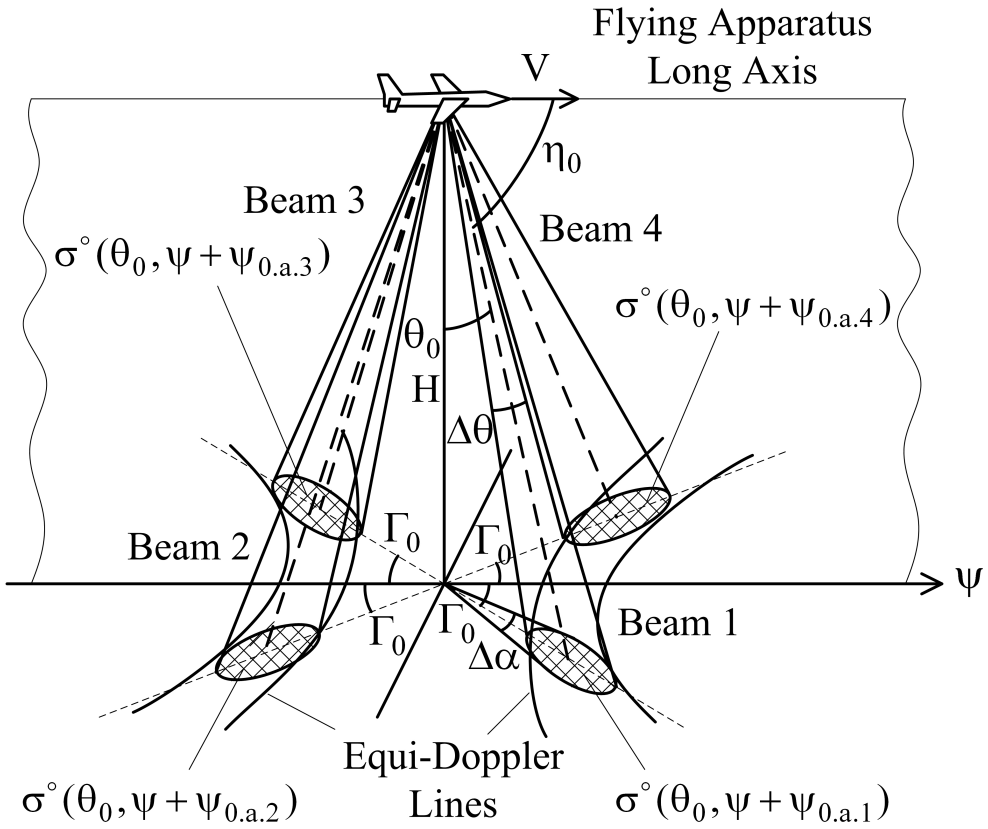

Fig. (1). Typical spatial location of the DNS beams: λ-configuration (beams 1, 2, and 3) and x-configuration (beams 1, 2, 3, and 4).

use a mounting angle of a beam axis in the inclined plane of somewhere between 65° and 80° [22]. The choice of a mounting angle of a beam axis in the horizontal plane Γ_0 depends on the desired sensitivity to drift, which tends to increase with increasing that mounting angle. For the typical Doppler-radar, mounting angles of a beam axis in the horizontal plane are of 15° to 45° [23].

The relationship among those mounting angles is [22]

$$\cos\eta_0 = \cos\Gamma_0 \cos\theta_0 . \quad (2)$$

Thus, the DNS multi-beam antenna allows selecting a power backscattered by the underlying surface from different directions, namely from directions corresponding to the appropriate beam relative to the aircraft course ψ, e.g. $\psi_{0.a.1}$, $\psi_{0.a.2}$, $\psi_{0.a.3}$, and $\psi_{0.a.4}$ in Fig. **(1)**. Each beam provides angular resolutions in the azimuthal and vertical planes, $\Delta\alpha$ and $\Delta\theta$ respectively.

Measurement of the Water Surface Backscattering Signature

As the azimuth NRCS curve can be obtained using the circle track flight for a scatterometer with an inclined one-beam fixed-position antenna [6], one beam of the DNS operating in the scatterometer mode can be used.

If the flying apparatus makes a horizontal rectilinear flight with the speed *V* at some altitude *H* above the mean sea surface, and the DNS has a roll-and-pitch-stabilized antenna system, the NRCS values obtained with beams 1, 2, 3, 4 would be $\sigma^\circ(\theta_0, \psi+\psi_{0.a.1})$, $\sigma^\circ(\theta_0, \psi+\psi_{0.a.2})$, $\sigma^\circ(\theta_0, \psi+\psi_{0.a.3})$, and $\sigma^\circ(\theta_0, \psi+\psi_{0.a.4})$ respectively.

Let the beam 1 be used to measure the water surface backscattering signature because both λ- and x-configured DNS have it. As a beam 1 axis is directed to the right side and its mounting angle in the vertical plane is not so far from nadir (at a straight flight), the circle flight with the left roll should be completed (Fig. **2**) [24].

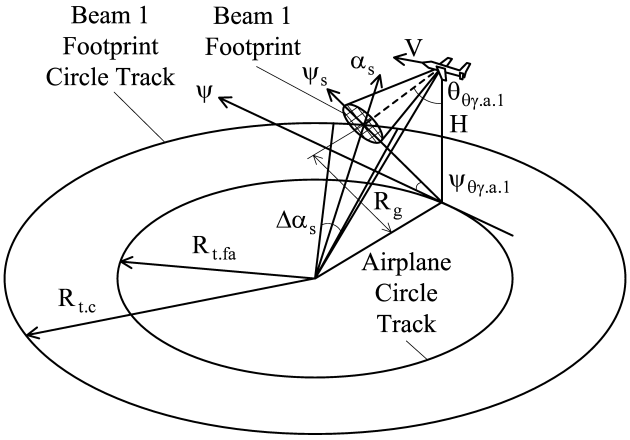

Fig. (2). Circle flight geometry for measurement of the water surface backscattering signature.

Let the DNS uses a fixed-antenna system (physically non-stabilized to the local horizontal) and the flying apparatus make the circle flight. Then, the values of the

incidence angle of the beam and the beam location in azimuthal plane will be not equal to the chosen design values, and so an actual incidence angle of the beam 1 $\theta_{\theta\gamma.a.1}$ and its actual azimuth direction $\psi_{\theta\gamma.a.1}$ relative to the aircraft current course (aircraft ground track) are as following [25]

$$\theta_{\theta\gamma.a.1} = \arctan\left(\sqrt{\tan^2(\arctan(\tan\theta_0 \sin\psi_{0.a.1}) + \gamma_{fa}) + \rightarrow} \right.$$
$$\left. \rightarrow \overline{\tan^2(\arctan(\tan\theta_0 \cos\psi_{0.a.1}) + \theta_{fa})}\right), \quad (3)$$

$$\psi_{\theta\gamma.a.1} = \begin{cases} \arctan\left(\dfrac{\tan(\arctan(\tan\theta_0 \sin\psi_{0.a.1}) + \gamma_{fa})}{\tan(\arctan(\tan\theta_0 \cos\psi_{0.a.1}) + \theta_{fa})}\right) \\ for\ \tan(\arctan(\tan\theta_0 \cos\psi_{0.a.1}) + \theta_{fa}) \geq 0 \\ \pi + \\ \arctan\left(\dfrac{\tan(\arctan(\tan\theta_0 \sin\psi_{0.a.1}) + \gamma_{fa})}{\tan(\arctan(\tan\theta_0 \cos\psi_{0.a.1}) + \theta_{fa})}\right) \\ for\ \tan(\arctan(\tan\theta_0 \cos\psi_{0.a.1}) + \theta_{fa}) < 0 \end{cases}, \quad (4)$$

where $\theta_{0.a.1}$ is the azimuthal mounting angle of the beam 1 axis relative to the aircraft course ψ, $\psi_{0.a.1} = \Gamma_0$, γ_{fa} is the roll angle of flying apparatus (right roll is positive), θ_{fa} is the pitch angle of flying apparatus (pull-up is positive).

Then, the current NRCS value obtained with the beam 1 is $\sigma^\circ(\theta_{\theta\gamma.a.1}, \psi + \psi_{\theta\gamma.a.1})$. The radius of the flying apparatus turn $R_{t.fa}$, the ground range R_g, and the radius of turn of the selected cell middle point $R_{t.c}$ are described by the following expressions obtained using the geometry of Fig. (**2**)

$$R_{t.fa} = \frac{V^2}{g\tan|\gamma_{fa}|}, \quad (5)$$

$$R_g = \frac{H}{\tan\theta}, \quad (6)$$

$$R_{t.c} = \sqrt{R_{t.fa}^2 + R_g^2 + 2R_{t.fa}R_g \sin\psi_{\theta\gamma.a.1}}, \quad (7)$$

where g is the acceleration of gravity, $g = 9.81\,\text{m/s}^2$.

The time of the airplane turn for 360° (360-degree turn) T_{360° is given by [26]

$$T_{360^\circ} = \frac{2\pi V}{g\tan|\gamma_{fa}|}. \quad (8)$$

Usually, the 360-degree azimuth space is divided into 72 or 36 sectors under the circle NRCS measurement. The azimuth size of a sector observed is 5° or 10°, respectively. A middle azimuth of the sector is the azimuth of the sector observed. The azimuth size of a sector relative to the center point of circle of the airplane track is $\Delta\alpha_s$, and the middle azimuth of a sector is α_s. The NRCS samples obtained from the sector and averaged over all measurement values in that sector give the NRCS value $\sigma^\circ(\theta_{\theta\gamma.a.1}, \psi_s)$ corresponding to the real observation azimuth angle of the sector ψ_s that is

$$\psi_s = \psi_{\psi_s} + \psi_{\theta\gamma.a.1} \pm 360^\circ, \quad (9)$$

where ψ_{ψ_s} is the flying apparatus course corresponding to the real observation azimuth angle of the sector.

Real observation azimuth angles of the sector beginning $\psi_{s.b}$ and of the sector ending $\psi_{s.e}$ are

$$\psi_{s.b} = \psi_s + \Delta\alpha_s/2 \pm 360^\circ, \quad (10)$$

$$\psi_{s.e} = \psi_s - \Delta\alpha_s/2 \pm 360^\circ, \quad (11)$$

The time of a sector view T_s and the number of samples N_s that can be obtained from the sector are represented by the following expressions

$$T_s = T_{360^\circ}\frac{\Delta\alpha_s}{360^\circ}, \quad (12)$$

$$N_s = \frac{T_s V}{0.5a}, \quad (13)$$

where a is the antenna length in the direction of flight.

Thus, to obtain an azimuth NRCS curve of the water surface at middle incidence angles under flying apparatus circle flight by the DNS operating in the scatterometer mode and using a fore-beam directed to the right side at a typical mounting angle in the vertical plane that is not so far from nadir at a straight flight, the measurement should be performed in accordance with a scheme of Fig. (**3**).

Measurement is started when a stable flight at the given altitude, speed of flight, roll and pitch has been established. Measurement is finished when the azimuth of the measurement beginning is reached. To obtain a greater number of NRCS samples for each sector observed several consecutive full circle turns for 360° may be done.

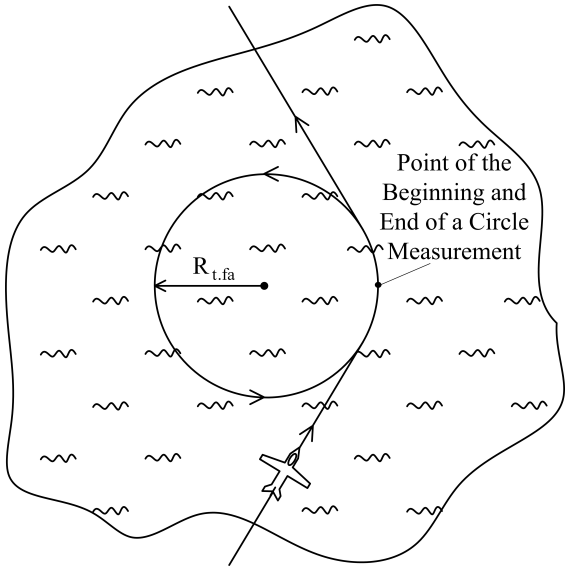

Fig. (3). Circle flight scheme for measuring the water surface backscattering signature.

Near-Surface Wind Vector Recovering

The NRCS of the water surface varies not only with the incidence angle but also as a function of the azimuth angle

relative to the up-wind direction. From (1), we can see that the NRCS azimuth curve has two maxima and two minima. The first (principal) maximum is located in the up-wind direction, the second maximum corresponds to the down-wind direction, and two minima are in cross-wind directions displaced slightly to the second maximum. With increase of the incidence angle, the difference between two maxima and the difference between maxima and minima become so significant (especially at middle incidence angles) that this feature can be used for retrieval of the wind direction over water [27].

In the general case, the problem of estimating the sea surface wind navigation direction ψ_w consists in finding the azimuth of the principal maximum of a curve of the backscattered signal intensity (direction of the principal maximum of the NRCS relative to the north $\psi_{\sigma^\circ_{\max}}$)

$$\psi_w = \psi_{\sigma^\circ_{\max}} \pm 180^\circ, \tag{14}$$

and the problem of deriving the sea surface wind speed consists in determination of a reflected signal intensity value from the up-wind direction or from some or all of the azimuth directions.

As the power reflected from the sea surface varies, to reduce the statistical fluctuation of detected power a number of independent samples for each azimuth direction (cell) are integrated. Required number of integrated samples from a cell to discriminate up-wind and down-wind NRCS values with the ratio of 0.5 dB is approximately 315. In the worst-case scenario when the NRCS values are not from up-wind and down-wind directions, not equal but differ by 0.2 dB or 0.1 dB, required number of integrated samples becomes 785 or 1565, respectively. So the use of the 360° azimuth NRSC curve will provide more precise wind vector estimation over water in comparison with the cases when the NRCS data only from some (three or four) azimuth directions are considered.

Let the sea surface backscattering be of the form (1). In case of the selected cell is narrow enough in the vertical plane, the NRCS model function for middle incidence angles (1) can be used without any correction for wind measurement while the azimuth angular size of a cell is up to $15^\circ - 20^\circ$ [28]. Then, the following algorithm to derive the wind vector over the water surface from measured NRCS data set can be proposed.

As the measured NRCS data set is discrete and in fact it is also a function of the wind speed, each NRCS value obtained $\sigma^\circ(\theta_{\gamma.a.1}, \psi_s)$ is considered now as $\sigma^\circ(U, \theta_{\theta\gamma.a.1}, \psi_{s.i})$, where $i = \overrightarrow{1, 360^\circ/\Delta\alpha_s}$. The wind speed can be found from the following equation

$$U = \left(\frac{\sum_{i=1}^{360^\circ/\Delta\alpha_s} \sigma^\circ(U, \theta_{\theta\gamma.a.1}, \psi_{s.i})}{\frac{360^\circ}{\Delta\alpha_s} a_0(\theta)} \right)^{1/\gamma_0(\theta)}. \tag{15}$$

To estimate the wind direction, at first the principal maximum value of the azimuth NRCS set

$$\sigma^\circ_{\max} = \max_{i=\overrightarrow{1, 360^\circ/\Delta\alpha_s}} \{\sigma^\circ(U, \theta_{\theta\gamma.a.1}, \psi_{s.i})\} \tag{16}$$

and the azimuth of the NRCS $\psi_{\sigma^\circ_{\max}}$ corresponding to it should be found. Then, more precise navigation wind direction can be found using least-squares procedure [29], when a larger NRCS set is used to estimate a location of the principal maximum value.

The function (1) at the measured wind speed value obtained from (15) is regarded to be the best approximation of sampled NRCS values within ±60° relative to its principal maximum in azimuth, and then, the least value of summation results by the least-squares procedure S_{min} can be written as follows

$$S_{\min} = \min_{j=\overrightarrow{0, \frac{360^\circ}{\Delta\alpha_s}}} \left\{ \sum_{i=j-\frac{60^\circ}{\Delta\alpha_s}}^{j+\frac{60^\circ}{\Delta\alpha_s}} \left(\sigma^\circ(U, \theta_{\theta\gamma.a.1}, \psi_{s.j}) - \sigma^\circ(U, \theta_{\theta\gamma.a.1}, \psi_i) \right)^2 \right\}. \tag{17}$$

The azimuth of the NRCS $\psi_{s.j}$ corresponding to the least value of summation results S_{min} will be $\psi_{\sigma^\circ_{\max}}$, and the wind direction can be found from (14).

RESULTS

The theoretical study has shown that the airborne DNS operating in the scatterometer mode can be used for measuring the water surface backscattering signature and estimating the near-surface wind vector over water in addition to its typical navigation application.

As the azimuth NRCS curve can be obtained by a scatterometer with an inclined one-beam fixed-position antenna using the circle track flight, one beam of the DNS can be used.

The beam should be pointed to the outer side of the aircraft turn to observe a greater area of the water surface and to obtain a greater number of independent NRCS samples. Since the mounting angle of the beam axis in the vertical plane is located not so far from nadir (at a straight flight), the circle flight with a small roll should be carried out to provide the azimuth NRCS curve measurement and near-surface wind vector estimation in the range of middle incidence angles.

Since coefficients in a geophysical model function are calculated by averaging NRCS values from a huge dataset obtained overall, the NRCS model function does not consider local wind, wave, temperature features and atmospheric precipitations. Together with the NRCS sampling variability and instrumental measurement errors an accuracy of the wind vector measurement better than the typical values mentioned above, cannot be expected without improvement of the geophysical model function taking into account some of those local factors. Also the DNS should provide the appropriate radiated power stability, and the

applicable range of altitudes should be defined for such measurements.

The principle considered and algorithms proposed in the paper can be used for the DNS enhancement, for designing an airborne radar system for operational measurement of the sea roughness characteristics and estimation of the wind speed and direction over water. They are also may be used for ensuring safe landing of amphibian aircraft on the water surface under search and rescue missions or fire fighting in the coastal areas and fire risk regions.

CONFLICT OF INTEREST

None declared.

ACKNOWLEDGEMENTS

I would like to express my sincere thanks to Hamburg University of Technology and The Ohio State University for their research opportunity provided, and to the German Academic Exchange Service (DAAD) and the Fulbright Program for their research fellowships.

REFERENCES

[1] Komen GJ, Cavaleri L, Donelan M, Hasselmann K, Hasselmann S, Janssen PAEM. Dynamics and modelling of ocean waves. Cambridge, UK: Cambridge University Press 1994; p.532.

[2] Moore RK, Fung AK. Radar determination of winds at sea. Proc IEEE 1979; 67(11): 1504-21.

[3] Melnik YuA. Radar methods of the Earth exploration. Moscow: Sovetskoye Radio 1980, p. 264 (in Russian).

[4] Chelton DB, McCabe PJ. A review of satellite altimeter measurement of sea surface wind speed: with a proposed new algorithm. J Geophys Res 1985; 90(C3): 4707-20.

[5] Feindt F, Wismann V, Alpers W, Keller WC. Airborne measurements of the ocean radar cross section at 5.3 GHz as a function of wind speed. Radio Sci 1986; 21(5): 845-56.

[6] Masuko H, Okamoto K, Shimada M, Niwa S. Measurement of microwave backscattering signatures of the ocean surface using X band and Ka band airborne scatterometers. J Geophys Res 1986; 91(C11): 13065-83.

[7] Wismann V. Messung der Windgeschwindigkeit über dem Meer mit einem flugzeuggetragenen 5.3 GHz Scatterometer. Dissertation zur Erlangung des Grades eines Doktors der Naturwissenschaften. Universität Bremen: Bremen, 1989; p. 119.

[8] Hildebrand PH. Estimation of sea-surface wind using backscatter cross-section measurements from airborne research weather radar. IEEE Trans Geosci Remote Sens 1994; 32(1): 110-7.

[9] Carswell JR, Carson SC, McIntosh RE, *et al*. Airborne scatterometers: investigating ocean backscatter under low- and high-wind conditions. Proc IEEE 1994; 82(12): 1835-60.

[10] Long MW. Radar reflectivity of land and sea. New York: Artech House 2001, p. 534.

[11] Plant WJ. Microwave sea return at moderate to high incidence angles. Waves Random Media 2003; 13(4): 339-54.

[12] Ward KD, Tough RJA, Watts S. Sea clutter: Scattering, the K distribution and radar rerformance. London: Institution of Engineering and Technology 2008, p. 450.

[13] Nielsen SN, Long DG. A wind and rain backscatter model derived from AMSR and SeaWinds data. IEEE Trans Geosci Remote Sens 2009; 47(6): 1595-606.

[14] Money DG, Mabogunje A, Webb D, Hooker M. Sea clutter power spectral lineshape measurements: Proceedings of Radar'97; Edinburgh, UK 1997: pp. 85-9.

[15] Ouchi K. A theory on the distribution function of backscatter radar cross section from ocean waves of individual wavelength. IEEE Trans Geosci Remote Sens 2000; 38(2): 811-22.

[16] Long DG, Donelan MA, Freilich MH, *et al*. Current progress in Ku-band model functions, Technical Report MERS 96-002. Provo, UT: Brigham Young University 1996; p. 88.

[17] Spencer MW, Graf JE. The NASA scatterometer (NSCAT) mission. Backscatter 1997; 8(4): 18-24.

[18] Nghiem SV, Li FK, Neumann G. The dependence of ocean backscatter at K_u-band on oceanic and atmospheric parameters. IEEE Trans Geosci Remote Sens 1997; 35(3): 581-600.

[19] Hans P. Auslegung und Analyse von satellitengetragenen Mikrowellensensorsystemen zur Windfeldmessung (Scatterometer) über dem Meer und Vergleich der Meßverfahren in Zeit- und Frequenzebene, Von der Fakultät 2 Bauingenieur- und Vermessungswesen der Universität Stuttgart zur Erlangung der Würde eines Doktor-Ingenieurs genehmigte Abhandlung. Institut für Navigation der Universität Stuttgart: Stuttgart 1987; p. 225.

[20] Askari F, Donato T, Keller WC. Airborne scatterometer detection of winds and sea surface roughness changes across the Gulf Stream front. Remote Sens Environ 1995; 53(1): 31-45.

[21] Sosnovskiy AA, Khaymovich IA. Radio-electronic equipment of flying apparatuses. Moscow: Transport 1987; p. 256, (in Russian).

[22] Kayton M, Fried WR. Avionics navigation systems. New York: John Wieley & Sons 1997, p. 773.

[23] Kolchinskiy VYe, Mandurovskiy IA, Konstantinovskiy MI. Autonomous Doppler facilities and systems for navigation of flying apparatuses. Moscow: Sovetskoye Radio 1975, p. 432, (in Russian).

[24] Nekrasov A. Airborne Doppler navigation system application for measurement of the water surface backscattering signature. In: Wagner W, Székely B, Eds. ISPRS TC VII Symposium – 100 Years ISPRS, Vienna, Austria, 2010, Vol. XXXVIII, Part 7A, pp. 163-8.

[25] Nekrassov A. Decrease of observation time and influence of flying apparatus list-tangage instability in measurement of sea surface wind vector: Proceedings of 5th International Conference on Remote Sensing for Marine and Coastal Environments, San Diego, California, USA; vol. 2, 1998; pp. 514-9.

[26] Mamayev VYa, Sinyakov AN, Petrov KK, Gorbunov DA. Air navigation and elements of navigation calculations. Saint Petersburg: GUAP 2002, p. 256 (in Russian).

[27] Ulaby FT, Moore RK, Fung AK. Microwave remote sensing: Active and passive, Volume 2: Radar remote sensing and surface scattering and emission theory. London: Addison-Wesley 1982, p. 1064.

[28] Nekrassov A. Sea surface wind vector measurement by airborne scatterometer having wide-beam antenna in horizontal plane: Proceedings of IGARSS'99, Hamburg: Germany 1999; pp. 1001-3.

[29] Bronshtein IN, Semendyayev KA. A guide book to mathematics. Frankfurt: Verlag Harri Deutsch 1973, p. 783.

Received: December 13, 2011 Revised: December 31, 2011 Accepted: January 01, 2012